Available online at www.sciencedirect.com
ScienceDirect
Journal of Environmental Sciences 2011, 23(9) 1424–1430
JOURNAL OF ENVIRONMENTAL SCIENCES
ISSN 1001-0742
CN 11-2629/X
www.jesc.ac.cn

Atmospheric mercury over the marine boundary layer observed during the third China Arctic Research Expedition

Hui Kang, Zhouqing Xie*

Institute of Polar Environment, University of Science and Technology of China, Hefei 230026, China. E-mail: zqxie@ustc.edu.cn

Received 22 November 2010; revised 08 March 2011; accepted 25 March 2011

Abstract

TGM measurements on board ships have proved to provide valuable complementary information to measurements by a ground based monitoring network. During the third China Arctic Research Expedition (from July 11 to September 24, 2008), TGM concentrations over the marine boundary layer along the cruise path were *in-situ* measured using an automatic mercury vapor analyzer. Here we firstly reported the results in Japan Sea, North Western Pacific Ocean and Bering Sea, where there are rare reports. The value ranged between 0.30 and 6.02 ng/m^3 with an average of (1.52 ± 0.68) ng/m^3, being slightly lower than the background value of Northern Hemisphere (1.7 ng/m^3). Notably TGM showed considerably spatial and temporal variation. Geographically, the average value of TGM in Bering Sea was higher than those observed in Japan Sea and North Western Pacific Ocean. In the north of Japan Sea TGM levels were found to be lower than 0.5 ng/m^3 during forward cruise and displayed obviously diurnal cycle, indicating potential oxidation of gaseous mercury in the atmosphere. The pronounced episode was recorded as well. Enhanced levels of TGM were observed in the coastal regions of southern Japan Sea during backward cruise due primarily to air masses transported from the adjacent mainland reflecting the contribution from anthropogenic sources. When ship returned back and passed through Kamchatka Peninsula TGM increased by the potential contamination from volcano emissions.

Key words: total gaseous mercury; atmosphere; marine boundary layer; Japan Sea; North Western Pacific Ocean; Bering Sea

DOI: 10.1016/S1001-0742(10)60602-X

Citation: Kang H, Xie Z Q, 2011. Atmospheric mercury over the marine boundary layer observed during third China Arctic Research Expedition. Journal of Environmental Sciences, 23(9): 1424–1430

Introduction

Mercury in the atmosphere results from numerous anthropogenic and natural processes (Aspmo et al., 2006). Natural emissions of mercury come from the oceans, crustal outgassing, volcanoes, evasion from surfacial soils, water bodies, wild fires, and geothermal sources (Schroeder et al., 1998; Mason et al., 2001). Anthropogenic sources include coal combustion, waste incineration, metal smelting, refining and manufacturing and gold mining (Schroeder and Munthe, 1998; Schroeder and Markes, 1994). It is estimated that two-thirds of the present mercury emission are directly or indirectly of anthropogenic origin (Mason et al., 1994).

Atmospheric mercury is speciated into gaseous elemental mercury (GEM), reactive divalent mercury (RGM) and particulate mercury (PHg). GEM can be transported over long distances because of the long lifetime with 0.5–2 years. Therefore, mercury can affect ecosystems on local, regional, and global scales. Global modeling studies indicate that 21%–24% of mercury deposition to North America is of Asian origin, compared to 30%–33% of North American origin (Seigneur et al., 2004; Travnikov, 2005).

Several observational studies have detected long-range transport of mercury from Asia. Aircraft measurements from sea level to ca. 7000 m during the 2001 ACE-Asia campaign found mercury to be well correlated with other pollutants in plumes over the western Pacific Ocean (Friedli et al., 2004). The highest concentrations of TGM were observed in the East China Sea (ca. 6.3 ng/m^3), the Sea of Japan (ca. 3 ng/m^3) and in the North Pacific Ocean (Miyake Jima volcano plume ca. 3.7 ng/m^3, and industrial source, ca. 3 ng/m^3). At a ground-based site in Okinawa, Japan, the concentrations of GEM were also measured and found to significantly correlate with the enhanced levels of CO, indicating the impact of anthropogenic emissions (Jaffe et al., 2005; Strode et al., 2008). In addition to the role of source, modeling results suggested atmospheric chemistry of mercury may influence on the levels of TGM, e.g., seasonal variation of TGM at northern mid-latitude was found to consistent with a photochemical oxidation of Hg^0 partly balanced by photochemical reduction of Hg^{2+} (Selin et al., 2007).

Although there are land-based and aircraft observations,

* Corresponding author. E-mail: zqxie@ustc.edu.cn

there are rare reports on TGM over the marine boundary layer in East Asia. In 1977–1980, marine atmospheric mercury was measured on board ship during the north-south traverses of Atlantic Ocean and the cruises over the Atlantic Ocean were repeated in 1990, 1994, 1996 and 1999–2001 (Slemr and Langer, 1992; Slemr et al., 1995; Slemr, 1996; Temme et al., 2003; Harris et al., 1992). The results suggested that the background concentration of TGM in the lower troposphere is generally around 1.7 and 1.3 ng/m^3 respectively, of the Northern Hemisphere and the Southern Hemisphere (Fitzgerald, 1995). More recently, Fu et al. (2010) measured gaseous mercury (GEM), surface seawater total mercury (THg), methyl mercury (MeHg) and dissolved gaseous mercury (DGM) in the South China Sea on board ship, revealing that high concentrations of GEM emitted from south China and Indochina peninsula. Obviously, TGM measurements on board ships proved to provide a valuable complementary information to measurements by a ground based monitoring network since they show a large-scale distribution and can provide information about sources of mercury and its long-range transport in areas not covered by the present monitoring network (Temme et al., 2003).

In this article, we firstly reported the results of TGM in the marine boundary layer in Japan Sea, Northwest Pacific Ocean and Bering Sea on board the Research Vessel (Xuelong) along the cruise path during the third China Arctic Research Expedition (from July 11 to September 24, 2008). TGM over the Arctic Ocean will be reported elsewhere.

1 Materials and methods

Highly time-resolved TGM measurements were carried out aboard a China Research Vessel Xuelong during the third China Arctic Research Expedition (CHINARE) in 2008. The ship departed from Shanghai, China (31.2°N, 121.3°E) on July 11, 2008, and passed through Bering Strait to the Arctic Ocean on August 1, 2008 and then carried out marine investigation in the Arctic Ocean for approximately 40 days. On September 9, 2008 the ship finished the Arctic investigation and passed through Bering Strait again. It arrived in Shanghai on 24 September. The track of the cruise is shown in Fig. 1, which covered East China Sea, Yellow Sea, Japan Sea, Okhotsk Sea, Bering Sea and the Arctic Ocean. During the cruise, all TGM data were quasi-continuously measured using an automatic Mercury Vapor Analyze (model 2537B, Tekran Inc., Toronto, Canada). The Tekran analyzer was installed at clean laboratory of the ship. Sampling line made of teflon (1/4″ o.d.) through an inlet outstretch the uppermost deck at the foreside to avoid the contamination from ship emissions. There is a heated layer outside the line which can control its temperature at 50°C and maintain its dryness. A downword funnel at sampling line inlet protected the collectors from rain and sea water droplets.

Tekran analyzer trapped mercury from air flow by amalgamating it on a gold cartridge, and then thermally desorbed from the gold cartridge, after that mercury

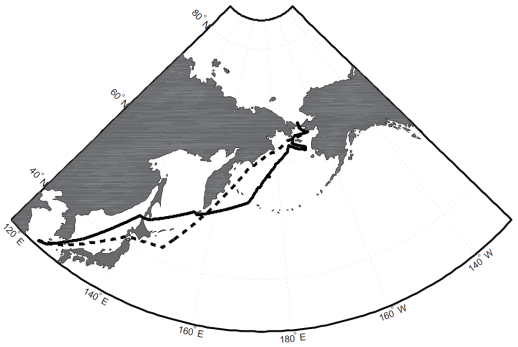

Fig. 1 Sketch map for the round-trip cruise between Shanghai and Bering Sea during the third China Arctic Research Expedition (CHINARE). Solid line represented forward cruise and dot line represented backward cruise.

was detected using cold vapor atomic fluorescence spectroscopy (CVAFS). There are two gold cartridges ('A' and 'B') in parallel flow paths, which were cycled between a concentration state and an analysis state to allow continuous sampling from 2.5 to 360 min. In this article, Tekran 2537B continued to measure TGM with a 5-min integrated sampling frequency. During the 5-min sampling period the air flows at a rate of 1.5 L/min through a 0.45-μm PTFE filter in front of the inlet before entering the analyzer to prevent sea salt aerosols. Tekran 2537B performed automated recalibrations for Hg^0 every 24 hr using an internal permeation source. The TGM detection limit in this operation mode is lower than 0.1 ng/m^3. The concentrations are reported in ng/m^3 (STP) at 273.16 K and 1013 mbar as standard temperature and pressure, respectively. As suggested by Temme et al. (2003), the measurements by the Tekran instrument represent the total gaseous mercury for this case as both elemental mercury and gaseous mercury compounds were collected on the gold collectors and transformed to elemental mercury during the amalgamation and thermal desorption.

Meteorological data with 5 min-averaged value including air temperature, relative humidity, wind direction and speed were obtained from forecast center of R/V Xuelong. According to the HYSPLIT model from NOAA-ARL (Draxier and Hess, 1998), 5-day backward trajectories were calculated in ensemble forms which calculated 27 trajectories from a selected starting point (Fain et al., 2009). Each member of the trajectory ensemble was calculated by offsetting meteorological data by one meteorological grid point (1 degree) in the horizontal (both latitudinal and longitudinal) and 0.01 sigma units (250 m) in the vertical for the selected starting point (Fain et al., 2009). In addition, to identify the potential source of mercury, NASA's satellite natural fire and volcanic degassing information were obtained from the OMI Sulfur Dioxide Group (http://so2.umbc.edu.cn).

2 Results and discussion

2.1 General trends in total gaseous mercury

The cruise between Shanghai and Bering Strait was split into two periods, namely, CHINARE-I and CHINARE-

II leg, respectively. CHINARE-I carried out in departing route from 13 July to 1 August, and CHINARE-II occurred in return route from 9 to 20 September. Figure 2 represents the highly-time resolved data set of TGM concentrations in ambient air over two periods. TGM concentrations ranged between 0.30 and 6.02 ng/m^3 with an average of (1.52 ± 0.68) ng/m^3. TGM varied with the latitude change. For CHINARE-I leg, TGM fluctuated around 1.3 ng/m^3 south of latitude 39°N, then decreased under 1.0 ng/m^3 until 55°N. After that, TGM increased with the maximum value at 6.02 ng/m^3. There were some episodes observed between 56°N and 66°N. For CHINARE-II leg, TGM values were lower between 60°N and 66°N compared to those during CHINARE-I leg, to the contrary, the values were higher from 40°N to 60°N with some episodes around 40°N. The values were comparable within latitude 35°N and 40°N during two periods.

A statistical summary of the TGM measurements in this cruise together with the previous cruise investigations in the marine boundary layer (e.g., the North Pacific Ocean, Atlantic Ocean and Mediterranean Sea) is listed in Table 1. Obviously, TGM showed different. Our observations were lower than most of previous results. For example, measurements of TGM in Mediterranean Sea ranged between 0.40 and 11.2 ng/m^3 with an average of (1.90 ± 1.02) ng/m^3 (Sprovieri et al., 2003), GEM concentrations over the northern South China Sea ranged from 1.04 to 6.75 ng/m^3 with an average of (2.62 ± 1.13) ng/m^3 (Fu et al., 2010). Our results were comparable with those observed in North Atlantic within 54°N–85°N (Aspmo et al., 2006) and those observed by Xia et al. (2010), which firstly reported the results of TGM made on board the China Research Vessel Xuelong over the Pacific Ocean, Indian Ocean and Antarctic Ocean in 2007. The values ranged between 0.302 and 4.496 ng/m^3 with an average of (1.536 ± 0.785) ng/m^3 (Xia et al., 2010). There are no previous investigations performed in the marine boundary layer along the same cruise as this campaign. Compared with the previous reported via aircraft during the 2001 ACE-Asia field campaign, the highest concentration of TGM by aircraft were observed in Japan Sea (ca. 3 ng/m^3) and in North Pacific Ocean (Mikaye Jima volcano plume ca. 3.7 ng/m^3) (Friedli et al., 2004). At ground-based sites in Okinawa of Japan, Hg^0 concentration was (2.04 ± 0.38) ng/m^3 during spring 2004 (Jaffe et al., 2005). Obviously, both aircraft and land-based observations were higher than our results. Although the absolute value of TGM in this study was lower, the enhanced TGM were also observed in Japan Sea. Along this study cruise, Selin et al. (2007) recently modeled mercury values in surface air using GEOS-Chem gobal tropospheric chemistry model. The concentrations of gaseous mercury were lower than the aircraft values, but higher than our observations, indicating GEOS-Chem may overestimated mercury concentrations in this regions.

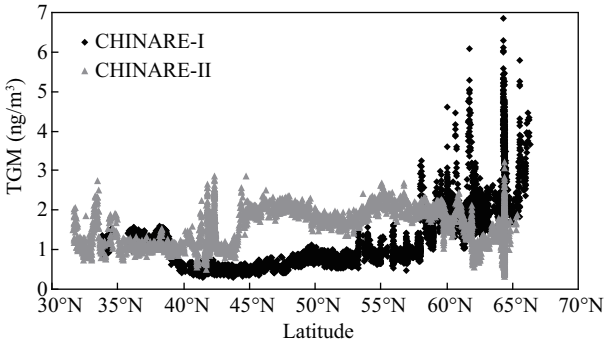

Fig. 2 Record of TGM concentrations during the period of CHINARE-I and CHINARE- II leg.

In view of spatial distribution of TGM, the sampling regions were geographically separated into Japan Sea, Okhotsk Sea and Bering Sea and further discussed in detail in the following sections. Briefly, a statistical summary of TGM measurements related to geographical regions are reported in Table 2.

2.2 Spatial distribution and potential sources of TGM

2.2.1 Japan Sea

The Research Vessel Xuelong navigated in Japan Sea between 13 and 15 July in CHINARE-I and between 18 and 20 September in CHINARE-II, respectively. TGM concentrations during two periods versus latitude are shown in Fig. 3. TGM ranged from 0.30 to 2.24 ng/m^3 with an average of 0.95 ng/m^3. In the range of 34°N–39°N, the concentration of TGM varied between 1.0 and 1.5 ng/m^3 and was comparable for CHINARE-I and CHINARE-II. Notably, TGM levels in the north of Japan Sea within the latitude 39°N–45°N were relatively higher during CHINARE-II than CHINARE-I. Especially, there were some episodes with high values up to 2.0 ng/m^3 observed around 41°N. As shown in Fig. 1, the backward

Table 1 Summary of the measurements of TGM and gaseous elemental mercury (GEM) over the marine boundary layer

Hg species	Cruise	Latitude	Mean (ng/m^3)	Range (ng/m^3)	Reference
TGM	October 1977	Atlantic 11°N–33°N	1.80	1.00–2.60	Temme et al., 2003a
TGM	Jan to Feb 1979	Atlantic 21°N–53°N	2.20	1.60–3.10	Temme et al., 2003a
TGM	23 Mar to 2 May 2004	Okinawa, Pacific	2.00	1.40–4.70	Jaffe et al., 2005
TGM	14 Jul to 9 Aug 2000	Mediterranean Sea	1.90	0.40–11.2	Sprovieri et al., 2003
GEM	15 Jun to 29 Aug 2004	North Atlantic 54°N–85°N	1.53	1.15–1.95	Aspmo et al., 2006
GEM		North Pacific 22°N–48°N	2.50	1.60–4.70	Laurier et al., 2003
TGM	18 to 20 Nov 2007	West Pacific 2°N–17°N	1.40	1.10–2.00	Xia et al., 2010
GEM	10 to 28 Aug 2008	South China Sea 17°N–22°N	2.62	1.04–6.75	Fu et al., 2010
TGM	Jul to Sep 2008	Pacific 30°N–66°N	1.52	0.30–6.02	This work

TGM: total gaseous mercury; GEM: gaseous elemental mercury.

Table 2 Statistical summary of TGM concentrations during the cruise (unit: ng/m^3)

	Location	Maximum	Minimum	Average	SD	No. of samples
	Whole cruise (except the Arctic Ocean)	6.02	0.30	1.52	0.68	4975
	Japan Sea	1.59	0.30	0.80	0.36	622
CHINARE-I	Okhotsk Sea	1.19	0.37	0.74	0.15	866
	Bering Sea	6.02	0.61	1.94	0.85	1012
	Japan Sea	2.24	0.70	1.14	0.23	486
CHINARE-II	Okhotsk Sea	2.88	0.52	1.71	0.43	1157
	Bering Sea	3.07	0.55	1.60	0.46	832

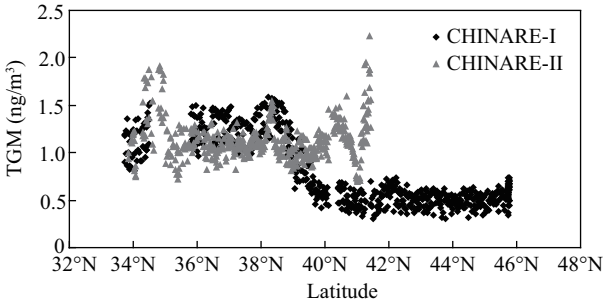

Fig. 3 TGM concentrations observed in Japan Sea.

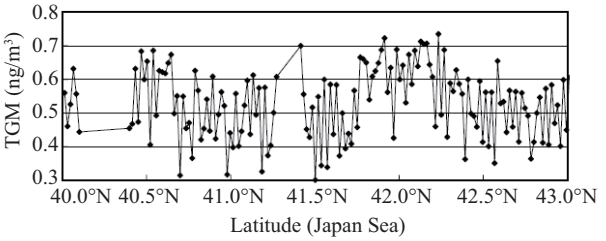

Fig. 5 Diurnal variations of TGM in Japan Sea.

cruise track was found to be more close to Japan Islands, indicating a potential anthropogenic contamination. One of episodes observed on September 17 was further selected to analyze in combination with five-day backward air trajectory. As shown in Fig. 4, this episode was characterized by the air masses mainly passing through Japan and Korea peninsula. These regions have intensive human activities including coal mining, steel production and oil industry, especially Seto Inland Sea industrial zone is one of the heavily industrialization in Japan. Jiang et al. (2006) has reported that large amounts of Hg will emit from industrial pollution.

In the north of Japan Sea it is interesting that TGM levels are much lower than 0.5 ng/m^3 for most of the time and display obviously diurnal cycle during CHINARE-I (Fig. 5), implying atmospheric mercury depletion events (AMDEs) may occur in this region. Previously, AMDEs only observed in the Springtime in the polar regions (Lu et al., 2001; Lindberg et al., 2001), until recently, Obrist et al. (2011) found that AMADE is also observed in the mid-latitude atmosphere. Potential reactions of Hg in the atmosphere have recently been summarized by Steffen et al. (2008). The primary reactions include the oxidation by O_3 (Pal and Ariya, 2004b), the OH radical (Sommar et al., 2001; Pal and Ariya, 2004a), H_2O_2 (Tokos et al., 1998) and reactive halogen species (Ariya et al., 2002) and Br atoms (Xie et al., 2008). Active halogen species such as Br/Cl will oxide the Hg^0 and produce reactive gaseous mercury (RGM) and then depletion of Hg^0 in the atmosphere (Xie et al., 2008). Sprovieri et al. (2003) has reported a diurnal cycle of the RGM concentration in the marine boundary layer along a 6000 km cruise path around the Mediterranean Sea and suggested that the potential oxidants may be OH. Recent reports proposed bromine-induced mercury oxidation may be an important source of mercury to the world's oceans (Obrist et al., 2011). However, there are no concurrent observations of trace gases in this study, further investigations in atmospheric chemistry in this region are thus necessary to explain the reaction mechanism.

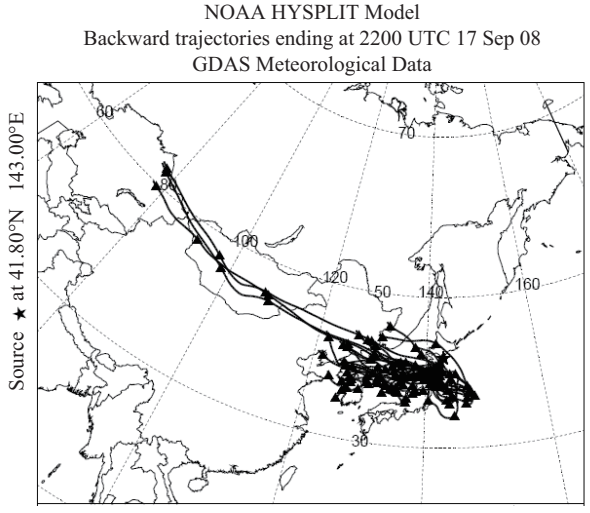

Fig. 4 Five-day backward trajectory on 17 September 2008.

2.2.2 Okhotsk Sea

The Research Vessel Xuelong passed through Okhotsk Sea and northwest Pacific on 15 to 18 July during CHINARE-I leg and on 13 to 18 September during CHINARE-II leg, respectively. The record of TGM in this region is shown in Fig. 6. TGM concentrations were very low and showed little variation around 0.7 ng/m^3 during CHINARE-I leg. While the values of TGM varied considerably from 0.52 to 2.88 ng/m^3 during CHINARE-II where the average value was much higher than CHINARE-I. Especially, TGM was high up to about 2.0 ng/m^3 within 45°N–56°N, higher than the background values of the Northern Hemisphere.

To identify the potential sources of TGM, wind-rose pattern was investigated during the sampling period. As shown in Fig. 7a1, during CHINARE-I forward cruise the

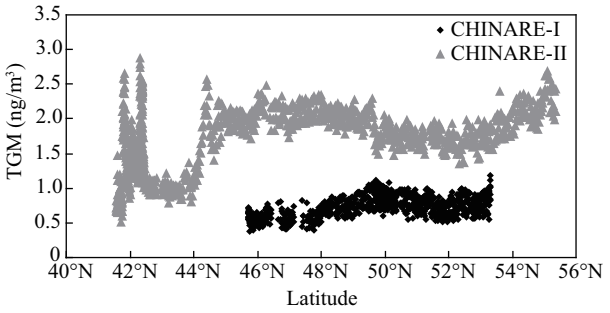

Fig. 6 TGM concentrations in Okhotsk Sea and North Western Pacific Ocean.

relative highest frequency of wind direction was almost from the bow, indicating that air-mass originated from the open sea (Fig. 1). The corresponding average TGM regarding to each direction is shown in Fig. 7a2 as well. Apparently, the marine air mass carried low concentration of TGM. During CHINARE-II backward cruise the path was very close to the coastal of Kamchatka Peninsula. The relative highest frequency of wind direction was almost from the up-right of the bow (Fig. 7b1), indicating that air-mass originated from the inland (Fig. 1). As shown in Fig. 7b2, the corresponding average TGM from this direction carried high level of TGM. It is well known that Kamchatka Peninsula has about 160 volcanoes, 29 of which are still active. Volcanoes are one of important natural sources of volatile mercury in the atmosphere. Gudmundsson et al. (1997) has found that the plume from a volcano eruption on Iceland at Vatnajokull area results in high level of TGM. To investigate the potential contamination of volcano eruption and/or degrassing in this region, we obtained the information of SO_2 concentration emitted from volcano by the NASA's satellite. As shown in Fig. 8, SO_2 column values were higher up to 0.6 and 2.0 DU at the northwest Pacific near Kamchatka Peninsula, indicating volcano emission really occurred. Hence, the relatively higher value of TGM observed in the backward cruise should be attributed to the emission from volcano

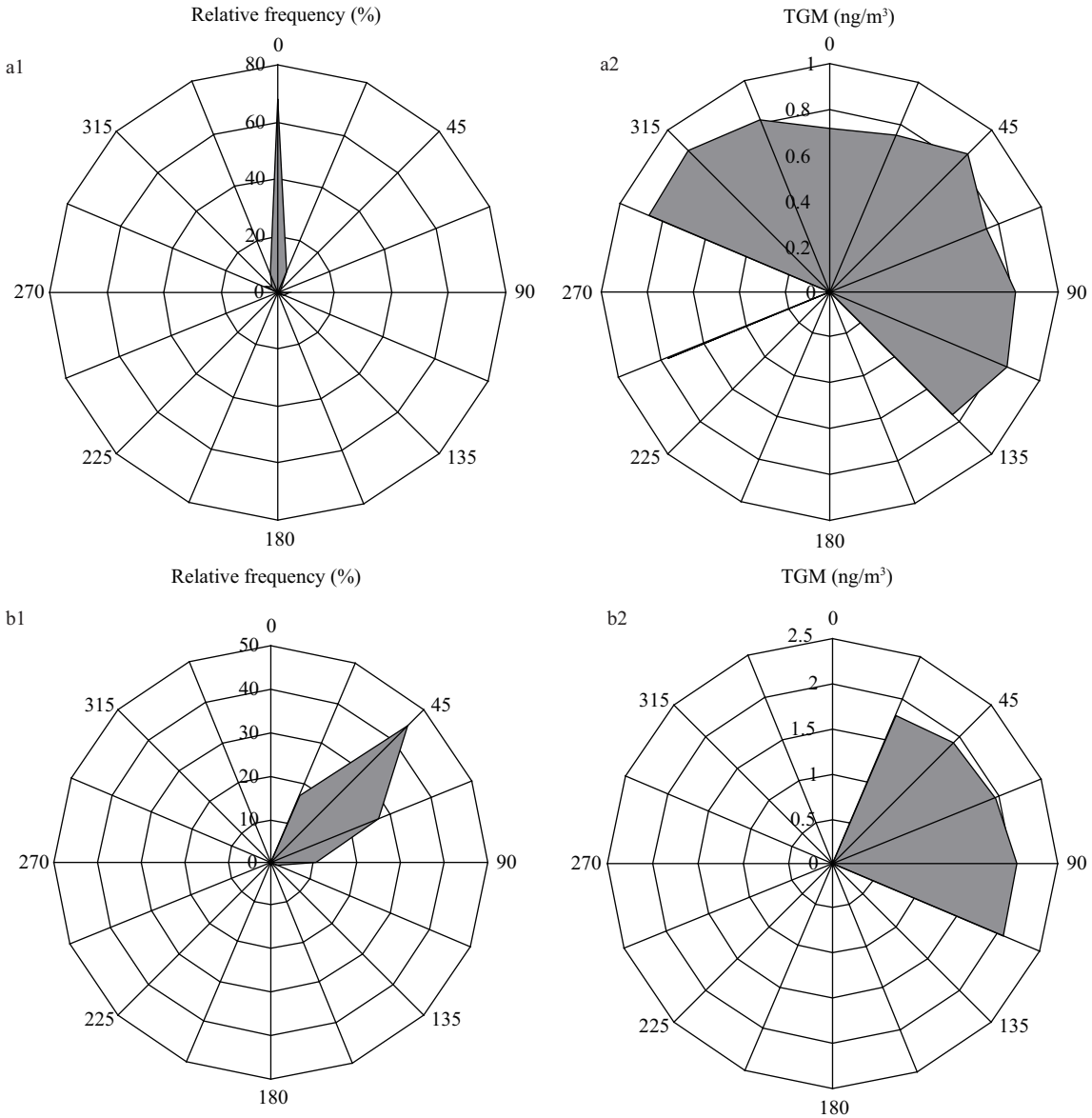

Fig. 7 Wind rose diagram (a1, b1) and the TGM concentration-wind direction (a2, b2) figure during CHINARE-I (a) and CHINARE-II (b). The relative wind direction of zero means air flow the bow.

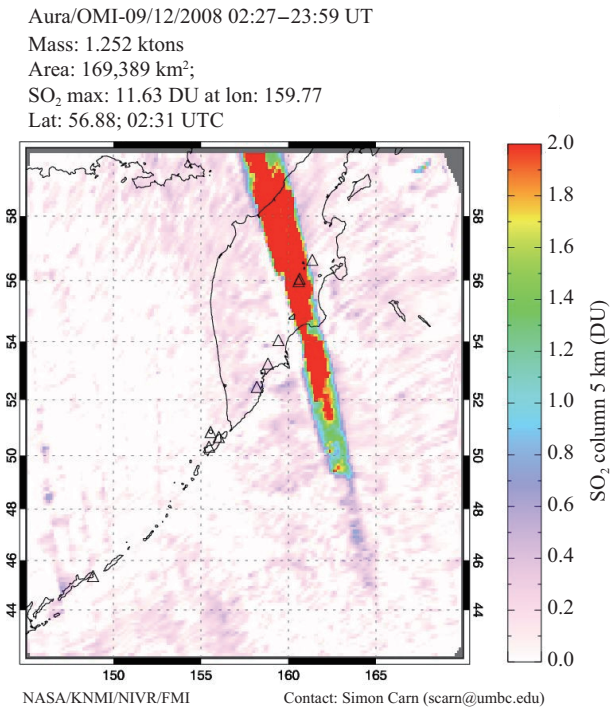

Fig. 8 SO_2 concentration emitted from volcano by the NASA's satellite on 12 September 2008.

eruption.

2.2.3 Bering Sea

The Research Vessel Xuelong navigated in Bering Sea between 18 July and 1 August during CHINARE-I, and 9 to 13 September during CHINARE-II, respectively. The concentration of TGM versus latitude over the two periods was shown in Fig. 9. During CHINARE-I, enhanced TGM occurred from 58°N to 66°N. The maximum value was higher up to 6.85 ng/m^3. Notably TGM changed abruptly within short time during this period, indicating local source contamination. While TGM concentration varied slightly during CHINARE-II. During the forward cruise the Research Vessel stopped frequently at marine station in Bering Sea to perform ocean investigation. The working time usually lasted for half of days at each station. Almost all of the episodes were observed during this period. The enhanced level of TGM during forward cruise was reasonable to be ascribed to the contamination by ship emission itself and can not represent the background value in Bering Sea. When the Research Vessel stopped at Nome harbor of America, TGM increased to about 4.0 ng/m^3 with the maximum value at 6.85 ng/m^3. Nome locates in Alaska, where it is a main port of USA. There are a large number of ships at this harbor. Ship emission will certainly increase the level of atmospheric mercury as well. Consequently, the data contaminated by ship emissions during the period of anchor station in Bering Sea were removed. The statistical average value of TGM was (1.79 ± 0.72) ng/m^3 (Table 2), which was comparable with the background values of Northern Hemisphere.

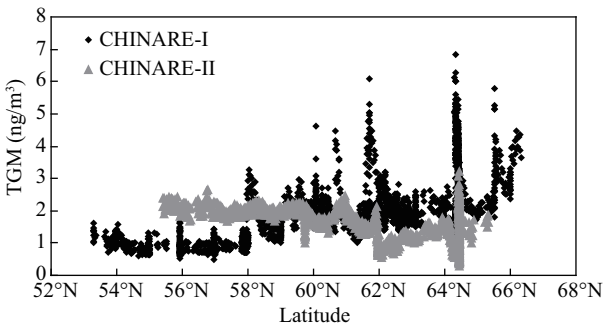

Fig. 9 TGM concentrations in Bering Sea.

3 Conclusions

During the third China Arctic Research Expedition (from July 11 to September 24, 2008), TGM concentrations over the marine boundary layer were measured using an automatic Mercury Vapor Analyze (model 2537B). Spatial distribution and potential sources of TGM in Japan Sea, Western North Pacific Ocean and Bering Sea were reported. The levels of TGM over the whole cruise ranged between 0.30 and 6.02 ng/m^3 with an average of (1.52 ± 0.68) ng/m^3, which was lower than the background value of Northern Hemisphere (1.7 ng/m^3). Obviously, TGM showed spatial and temporal variation. In the north of Japan Sea TGM levels during forward cruise were lower than 0.5 ng/m^3 for most of the time and displayed diurnal cycle, indicating potential oxidation of gaseous mercury in the atmosphere. The pronounced episode was recorded in the coastal regions of southern Japan Sea during backward cruise due primarily to air masses transported from the adjacent mainland reflecting the contribution from anthropogenic sources. When ship returned back and passed through Kamchatka Peninsula, volcano emission enhanced TGM levels.

Acknowledgments

This research was supported by the National Natural Science Foundation of China (No. 41025020, 40776001), the Knowledge Innovation Project of the Chinese Academy of Sciences (No. KZCX2-YW-QN506) and the Fundamental Research Funds for the Central Universities. The authors gratefully acknowledge the NOAA Air Resources Laboratory (ARL) for the provision of the HYSPLIT transport and dispersion model and/or READY website (http://www.arl.noaa.gov/ready.html) used in this publication. Fieldwork was supported by the International Polar Year Project from China Arctic and Antarctic Administration and performed during the third China Arctic Research Expedition.

References

Ariya P A, Khalizov A, Gidas A, 2002. Reactions of gaseous mercury with atomic and molecular halogens: kinetics, product studies, and atmospheric implications. *Journal Physical Chemistry A*, 106(32): 7310–7320.

Aspmo K, Temme C, Berg T, Ferrari C, Gauchard P, Fain X et al., 2006. Mercury in the atmosphere, snow and melt water ponds in the North Atlantic Ocean during Arctic Summer. *Environmental Sciences and Technology*, 40: 4083–4089.

Draxier R R, Hess G D, 1998. An overview of the HYSPLIT

4 modelling system for traiectories, dispersion and deposition. *Australian Meteorological Magazine*, 47: 295–308.

Fain X, Obrist D, Hallar A G, Cubbin I M, Rahn T, 2009. High levels of reactive gaseous mercury observed at a high elevation research laboratory in the Rocky Mountains. *Atmospheric Chemistry and Physics*, 9: 15641–15671.

Fitzgerald W F, 1995. Is mercury increasing in the atmosphere? The need for an atmospheric mercury network (AMNET). *Water Air Soil Pollution*, 80: 245–254.

Friedli H R, Radke L F, Prescott R, Li P, Woo J H, Carmichael G R, 2004. Mercury in the atmosphere around Japan, Korea, and China as observed during the 2001 ACE-Asia field campaign: measurements, distributions, sources, and implications. *Journal of Geophysical Research*, 109: D19S25,13.

Fu X W, Feng X B, Zhang G, Xu W H, Li X D, Yao H et al., 2010. Mercury in the marine boundary layer and seawater of the South China Sea: Concentrations, sea/air flux, and implication for land outflow. *Journal of Geophysical Research*, 115: D06303.

Gudmundsson M T, Sigmundsson F, Bjornsson H, 1997. Ice-volcano interaction of the 1996 Gjalpsuglacial eruption, Vatnajokull, Iceland. *Nature*, 389: 954–957.

Harris J M, Tans P P, Dlugokencky E J, Masarie K A, Lang P M, Whittlestone S et al., 1992. Variations in atmospheric methane at Mauna-Loa-Observatory related to long-range transport. *Journal of Geophysical Research*, 97: 6003–6010.

Jaffe D, Prestbo E, Swartzendruber P, Weiss-Penzias P, Kato S, Takami A et al., 2005. Export of atmospheric mercury from Asia. *Atmospheric Environment*, 39(17): 3029–3038.

Jiang G B, Shi J B, Feng X B, 2006. Mercury pollution in China. *Environmental Science and Technology*, 40(12): 3672–3678.

Laurier F J G, Mason R P, Whalin L, Kato S, 2003. Reactive gaseous mercury formation in the North Pacific Ocean's marine boundary layer: A potential role of halogen chemistry. *Journal of Geophysical Research*, 108: 4529.

Lindberg S E, Brooks S, Lin C J, Scott K, Meyers T, Chamber L et al., 2001. Formation of reactive gaseous mercury in the arctic: Evidence of oxidation of Hg^0 to gas-phase Hg-II compounds after arctic sunrise. *Water Air Soil Pollution*, 1: 295–302.

Lu J Y, Schroeder W H, Barrie L A, Steffen A, Welch H E, Martin K et al., 2001. Magnification of atmospheric mercury deposition to polar regions in springtime: The link to tropospheric ozone depletion chemistry. *Geophysical Reseatch Letters*, 28: 3219–3222.

Mason R P, Fitzgerald W F, Morel F M M, 1994. The biogeochemical cycling of elemental mercury-anthropogenic influences. *Geochimica et Cosmochimica Acta*, 58(15): 3191–3198.

Mason R P, Lawson N M, Sheu G R, 2001. Mercury in the Atlantic Ocean: factors controlling air-sea exchange of mercury and its distribution in the upper waters. *Deep Sea Research Part II*, 48(13): 2829–2853.

Obrist D, Tas E, Peleg M, Matveev V, Fain X, Asaf D et al., 2011. Bromine-induced oxidation of mercury in the mid-latitude atmosphere. *Nature Geoscience*, 4: 22–26.

Pal B, Ariya P A, 2004a. Gas-phase HO-initiated reactions of elemental mercury: kinetics and product studies, and atmospheric implications. *Environmental Science and Technology*, 38(21): 5555–5566.

Pal B, Ariya P A, 2004b. Studies of ozone initiated reactions of gaseous mercury: kinetics, product studies, and atmospheric implications. *Physical Chemistry Chemical Physics*, 6: 572–579.

Schroeder W H, Markes J, 1994. Measurements of atmospheric mercuryconcentrations in Canadian environment near Lake Ontario. *Journal of Great Lakes Research*, 20(1): 240–259.

Schroeder W H, Munthe J, 1998. Atmospheric mercury: an overview. *Atmospheric Environment*, 32(5): 809–822.

Seigneur C, Vijayaraghavan K, Lohman K, Karamchandani P, Scott C, 2004. Modeling the atmospheric fate and transport of mercury over North America: power plant emission scenarios. *Fuel Processing Technology*, 85: 441–450.

Selin N E, Jacob D J, Park R J, Yantosca R M, Strode S, Jaeglé L et al., 2007. Chemical cycling and deposition of atmospheric mercury: Global constraints from observations. *Journal of Geophysical Research*, 112: D02308, 14.

Slemr F, 1996. Trends in atmospheric mercury concentrations over the Atlantic Ocean and at the Wank Summit, and the resulting constraints on the budget of atmospheric mercury. In: In Global and Regional Cycles: Sources, Fluxes and Mass Balances (Baeyens W, Ebinghaus R, Vasiliev O, eds.). NATO-ASI-Series, Kluwer Academic Publishers, Dordrecht, The Netherlands. 33–84.

Slemr F, Junkermann W, Schmidt R W H, Sladkovic R, 1995. Indication of change in global and regional trends of atmospheric mercury concentrations. *Geophysical Research Letters*, 22: 2143–2146.

Slemr F, Langer E, 1992. Increase in global atmospheric concentrations of mercury inferred from measurements over the Atlantic Ocean. *Nature*, 355: 434–437.

Sommar J, Gardfeldt K, Stromberg D, Feng X B, 2001. A kinetic study of the gas-phase reaction between the hydroxyl radical and atomic mercury. *Atmospheric Environment*, 35(17): 3049–3054.

Sprovieri F, Pirrone N, Gardfeldt K, Sommar J, 2003. Mercury speciation in the marine boundary layer along a 6000 km cruise path around the Mediterranean Sea. *Atmospheric Environment*, 37: 63–71.

Steffen A, Douglas T, Amyot M, Ariya P, Aspmo K, Berg T et al., 2008. A synthesis of atmospheric mercury depletion event chemistry in the atmosphere and snow. *Atmospheric Chemistry and Physics*, 8: 1445–1482.

Strode S A, Jaeglé L, Jaffe D A, Swartzendruber P C, Selin N E, Holmes C et al., 2008. Trans-Pacific transport of mercury. *Journal of Geophysical Research*, 113: D15305.

Temme C, Einax J W, Ebinghaus R, Schroeder W H, 2003a. Measurements of atmospheric mercury species at a coastal site in the Antarctic and over the south Atlantic Ocean during polar summer. *Environmental Science and Technology*, 37(1): 22–31.

Temme C, Slemr F, Ebinghaus R, Einax J W, 2003b. Distribution of mercury over the Atlantic Ocean in 1996 and 1999–2001. *Atmospheric Environment*, 37(14): 1889–1897.

Tokos J J S, Hall B, Calhoun J A, Prestbo E M, 1998. Homogeneous gas-phase reaction of Hg with H_2O_2, O_3, CH_3I, and $(CH_3)_2S$: Implications for atmospheric Hg cycling. A*tmospheric Environment*, 32(5): 823–827.

Travnikov O, 2005. Contribution of the intercontinental atmospheric transport to mercury pollution in the Northern Hemisphere. *Atmospheric Environment*, 39(39): 7541–7548.

Xia C H, Xie Z Q, Sun L G, 2010. Atmospheric mercury in the marine boundary layer along a cruise path from Shanghai, China to Prydz Bay, Antarctica. *Atmospheric Environment,* 44(14): 1815–1821.

Xie Z Q, Sander R, Poeschl U, Slemr F, 2008. Simulation of atmospheric mercury depletion events (AMDES) during polar springtime using the MECCA box model. *Atmospheric Chemistry and Physics*, 8: 7165–7180.